Characterization of Crosslinked, Macroporous, Monosized Polymer Particles

ANNE KARI NYHUS,[1] STEINAR HAGEN,[2] ARVID BERGE[1]

[1] Department of Chemical Engineering, Norwegian University of Science and Technology, N-7034 Trondheim, Norway

[2] Amersham Pharmacia Biotech AS, PB 213, N-2001 Lillestrøm, Norway

ABSTRACT: Macroporous, monosized poly(*meta*-divinylbenzene) and poly(*para*-divinylbenzene) beads have been prepared by the two-step activated swelling method with toluene or 2-ethylhexanoic acid as pore-forming agents. The type of divinylbenzene isomer as well as the type of porogen has a large effect on both physical and chemical properties of the monodisperse beads. Large pores are obtained with 2-ethylhexanoic acid as porogen while beads prepared in the presence of toluene consist of only small pores and exhibit a shrinking behavior upon drying. The beads have considerable amounts of residual vinyl groups at the end of polymerization, as determined by bromination and Fourier transform IR analysis. The morphology and texture of the particles have been investigated by scanning electron microscopy and atomic force microscopy. © 2000 John Wiley & Sons, Inc. J Appl Polym Sci 76: 152–169, 2000

Key words: monosized polymer particles; poly(divinylbenzene); morphology; macroporosity

INTRODUCTION

Techniques for the preparation of macroporous polymers were developed almost 40 years ago.[1–3] Porous structures are typically formed during the copolymerization of mixtures containing a divinyl monomer and inert porogens.[1–4]

Polymer beads are usually produced by suspension polymerization in which stirring provides some control of the average size of the droplets and the resulting beads.[5] This technique affords beads with a broad particle size distribution. In order to optimize the performance of the beads,

the two-step activated swelling method has been applied to the preparation of uniformly sized macroporous particles.[6,7]

The chemistry of the copolymerization together with the relationship between the structural characteristics of the polymer and its properties have been the subject of many studies.[3,8,9] Such an understanding needs a precise knowledge of the chemical microstructure, the porous texture, the swelling properties, the internal heterogeneity of the support, and the distribution of its active groups.

When the polymerization starts in a small droplet in the presence of a poor solvent for the polymer, the porous texture formation follows a three-stage mechanism. The agglomeration of polymer chains to give nuclei (5–20 nm) takes place at first followed by the formation of microspheres (60–500 nm), and finally agglomerates (10,000–100,000 nm).[1,2,4,10] Very small pores (50–150 Å) are located in between the nuclei, and

these pores are mainly responsible for the high surface area. In between the microspheres, there is a second family of intermediate pores (200–500 Å) and a third family of large pores is located between the agglomerates. The two successive steps in the formation of the porous texture include agglomeration of crosslinked microspheres and formation of the macroporous structure. This results in a rather strongly cohesive structure of the polymer matrix with a low degree of swelling. During the polymerization, the solvating power of the liquid medium is continuously decreasing because of the consumption of the monomer, and at a certain point the solvent medium is not a solvent for the polymer formed, which then precipitates.

When the polymerization is run in the presence of an inert diluent that is a good swelling liquid for the polymer, two levels of particle substructure instead of three, as discussed above, are formed. The porous texture is built up of rather large nuclei (20–50 nm) and their agglomerates, but no microspheres.[3,11] Under such conditions high surface areas in excess of 500 m[2]/g with a narrow distribution of very small pores (100 Å) are obtained.[12] The quality of the solvent medium does not change much during the course of the polymerization. When good solvents are used, the polymer chains remain dissolved in the mixture for a longer time prior to phase separation and the lightly crosslinked network is highly swollen by the solvent.

It is known that an increase in the fraction of crosslinking monomer generally leads to porous structures with larger surface areas and smaller pore sizes.[1,4] The phase separation takes place at a lower monomer conversion for systems with a high fraction of crosslinker. Both the absorption of monomers in the nuclei and the coalescence of the nuclei are limited as a result of their crosslinking. Thereby, the number of smaller individual nuclei remains large and smaller microspheres persist.

For a spherically symmetrical system, the relationship between microgel diameter and the total specific surface area (S_g) is given by[13]

$$S_g = \frac{6}{\rho_s D} \qquad (1)$$

where S_g is in units (m[2]/g), ρ_s is the skeletal density of the particle mass (g/cm^{3}), and D is the diameter in μm of the element (microgel) provid-

ing the surface. The size of the microspheres or nuclei can be calculated from the measured specific surface area and skeletal density, assuming that they are relatively uniform in size. A filmed monolayer of poly(divinylbenzene) would have a specific surface area of 2313 m[2]/g on each side of the filmed layer at an assumed packing fraction of 1.0.[13]

In the present study, macroporous, monodisperse polymer particles of 33 μm have been prepared from pure *meta-* and *para-*divinylbenzene (DVB) to avoid the compositional heterogeneity of the copolymer made from commercial DVB.[6,7,9,14,15] Two different types of pore-forming agents (toluene *vs* 2-ethylhexanoic acid) have been used to investigate their influence on the porous texture. The main focus was on the morphological aspects and the pore size distribution. The characterization techniques used include: pore size distribution and total pore volume by nitrogen desorption isotherm and mercury porosimetry, specific surface area by the Brunauer–Emmett–Teller (BET) isotherm, inverse size exclusion chromatography (ISEC), scanning electron microscopy (SEM), atomic force microscopy (AFM), and diffuse reflectance Fourier Transform IR spectroscopy (DRIFT).

EXPERIMENTAL

Materials

Isophthalaldehyde (98%), terephthalaldehyde (98%), methyltriphenylphosphonium bromide (98%), potassium *tert*-butoxide (97%), tetrahydrofuran (99%), hexane (99%), sodium chloride, and sodium dodecyl sulphate (99%) were purchased from Fluka Chemica (Chemie AG, CH-9470 Buchs). Toluene (99%), 2-ethylhexanoic acid (98%), tetrachloromethane (99%), acetone (99%), methanol (99%), isopropylalcohol (98%), bromine (98%), and 4-tert-butyl pyrocatechol (98%) were purchased from Merck Darmstadt, and used as received. Hexylbenzene and pentylbenzene were purchased from Sigma Aldrich (D-89555 Steinheim). Dioctanoyl peroxide was bought from Akzo Chemicals (3800 AE Amersfoort).

Preparation of *meta*-Divinylbenzene and *para*-Divinylbenzene

Pure *meta*-DVB and *para*-DVB were synthesized by the Wittig reaction as reported earlier by us.[15]

Table I   Composition and Amount of Residual Vinyl Groups in Monodisperse Particles and Bulk Samples

Sample	Monomer	Porogen	Type	Residual Vinyl Groups[e] (mmole C = C/g)	Conversion[f] (%)
A1E	*meta*-DVB[a]	Toluene	MPP[c]	2.75 ± 0.14	64.3
A2E	*para*-DVB[a]	Toluene	MPP[c]	3.49 ± 0.17	54.7
A4E	*meta*-DVB[a]	2-EHA[b]	MPP[c]	2.76 ± 0.14	64.2
A5E	*para*-DVB[a]	2-EHA[b]	MPP[c]	3.52 ± 0.18	54.3
A14	*meta*-DVB[a]	2-EHA[b]	BP[d]	2.04 ± 0.10	73.5
A15	*para*-DVB[a]	2-EHA[b]	BP[d]	3.17 ± 0.16	58.8
A16	*meta*-DVB[a]	Toluene	BP[d]	2.71 ± 0.13	64.8
A17	*para*-DVB[a]	Toluene	BP[d]	3.71 ± 0.18	51.8

[a] DVB: divinylbenzene.
[b] EHA: 2-ethylhexanoic acid.
[c] MPP: Monodisperse polymer particles.
[d] BP: bulk samples.
[e] Determined by bromination.
[f] Conversion of second double bonds.

Preparation of Monodisperse Polymer Particles

Four types of macroporous, monodisperse polymer particles of diameter 33 μm were prepared by the two-step activated swelling method.[6,7] The particle matrices were homopolymers from *meta*-DVB and *para*-DVB. The monomers were polymerized by the use of dioctanoyl peroxide as initiator. The porosity was obtained using toluene and 2-ethylhexanoic acid as porogen, and the monomer: porogen ratio for all the particle types was 1:2.3 (v/v). The total porogen content was 70% by volume. The composition of the particles is given in Table I.

Preparation of Bulk Samples

Four types of macroporous bulk samples were prepared from *meta*-DVB and *para*-DVB. The porogens used were toluene and 2-ethylhexanoic acid. The monomer: porogen ratio for all polymer types was 1:2.3 (v/v). The total porogen content was 70% by volume. The composition of the bulk samples is given in Table I. The initiator dioctanoyl peroxide, monomer, and porogen were mixed, added into glass tubes, and placed in a thermostated bath. The glass vials were of 9-mm diameter and 30-mm length. The polymerization was run for 22 h at 70°C. The prepared bulk samples (0.5 g) were crushed into powder in a mortar and washed with isopropylalcohol (100 mL), methanol (100 mL), and acetone (100 mL). The polymers were dried overnight at 50°C.

Reaction of Porous Samples with Bromine

Residual vinyl groups in the four types of monodisperse polymer particles were brominated to various bromination degrees using 0.25, 0.50, 0.75, and 1.00 mmole Br_2/mmole C=C. The residual vinyl group content in the final samples at the end of the polymerization was determined by reaction with tenfold excess (10.00 mmole Br_2/mmole C=C) of bromine. The bromine was dissolved in tetrachloromethane and added to the dry porous samples to give dibromide.[16–18] The amount of dibromide corresponds to the amount of residual vinyl groups. The reaction was run overnight in the dark at room temperature. The brominated particles (0.4 g) were washed with tetrachloromethane (15 mL) and acetone (15 mL). The particles were dried over night at 50°C. The bromine bound to the polymer matrices was liberated by fusion at 550°C in the presence of Na_2CO_3. Finally, bromide was determined by titration with $AgNO_3$.[15]

Characterization

Pore Size Distribution and Specific Surface Area

The specific surface area was determined by the BET isotherm, and the pore size distribution of small pores was calculated from the nitrogen desorption isotherm using a Carlo Erba Sorptomatic 1900 instrument.[19,20] The mercury intrusion method was applied for the determination of me-

dium and large pores using a Carlo Erba Porosimeter 2000 instrument and a Carlo Erba Macropores Unit 120.[21]

Inverse Size Exclusion Chromatography

A Waters high performance liquid chromatography (HPLC) system consisting of two HPLC pumps (510 and 590), a 717 plus autosampler and a 486 UV detector controlled by Millenium 2010 software was applied for ISEC. In most cases, the particles were packed into 34×10mm i.d. glass columns from a methanol suspension. A few samples were also run in steel columns of dimension 150×46mm i.d. ISEC was carried out in tetrahydrofuran using toluene, pentylbenzene, hexylbenzene, and several polystyrene standards with molecular weights ranging from 580 to $14 \cdot 10^6$ g/mole to determine the calibration curve. The flow was 0.2 mL/min. The peaks were monitored at 254 nm, and the distribution coefficients K_d were calculated according to

$$K_d = (V_R - V_O)/V_P \qquad (2)$$

where V_R is the retention volume of a standard, V_0 is the void volume of the packed column (elution volume of the largest polystyrene standard), and V_P is the total pore volume available for the penetration of toluene.

Scanning Electron Microscopy

The morphology and the texture of the polymer particles in the dry state were investigated by SEM using a Zeiss Digital Scanning Microscope 940.

Atomic Force Microscopy

The three-dimensional images of the particle surfaces were obtained using tapping mode atomic force microscopy on a Nanoscope III from Digital Instruments. Nanosensors pointprobes for tapping mode (Si tips) were applied. The lateral resolution is quite comparable for the contact and noncontact AFM. Moreover, the pressure force applied to the sample in TM AFM is much lower than in the contact AFM. Plane Fit is used for both the x and y axes. All images presented were obtained in the tapping mode over a representative $1 \times 1 \ \mu m^2$ area. The particle surfaces were compared by means of roughness parameters, such as the mean roughness R_a, the root mean square (rms), of the Z $data$ R_q and R_{max}. These

parameters are defined by Lehmani et al.[22] The R_a factor is the mean value for the surface relative to the centerplane. This factor is independent of the correction for curvature or inclination. R_{max} is the height difference between the highest and lowest plane points on the surface relative to the mean plane. R_q is the standard deviation of the Z values within the given area.

Fourier Transform IR Spectroscopy (FTIR)

DRIFT spectroscopy was carried out using a PE 1720X FT-IR spectrometer equipped with a Spectra-Tech diffuse reflectance accessory. The samples of polymer particles were mixed with KCl to give 1% w/w mixtures. These were then packed into standard sample cups. A total of 50 scans using a resolution of 4 cm^{-1} were taken. The spectra were transformed into Kubelka Munk units using Perkin Elmer Spectrum for Windows 96 Software.

Swelling Measurements

The volume swelling of porous monosized polymer particles was calculated from optical micrographs of dry and swollen particles using a Zeiss Axioskop equipped with a Sony CCD/RGB Video Camera connected to a Sony Graphic printer UP 860 CE.

RESULTS AND DISCUSSION

Residual Vinyl Group Content

The composition and the amount of residual vinyl groups determined by bromination of the monosized polymer particles and the bulk samples are given in Table I. The theoretical value of residual vinyl groups of a linear polymer of DVB is 7.7 mmole vinyl/g. Table I shows that the conversion of the second double bonds is in the range 52–74% at the end of the polymerization resulting in intermolecular and intramolecular crosslinking. It is found that polymer matrices made from *para*-DVB have a higher amount of unpolymerized double bonds than those from *meta*-DVB, a result that seems to be independent of the porogen. It is seen that monodisperse particles prepared from the same isomeric type of monomer have equal amounts of residual vinyls applying either of the two porogens. The bulk samples, however, prepared from similar DVB isomers show some minor differences in vinyl content with change of

Table II   Swelling of Monodisperse Polymer Particles

Sample	Swelling in Toluene (% v/v)[a]	Swelling in SDS[b] Solution (% v/v)[a]
A1E	27	11.5
A2E	58	39
A4E	0	0
A5E	0	0

[a] % (v/v) swelling = $(V_{sp} - V_p)/V_p \cdot 100$, where V_{sp} is the volume of swollen particle and V_p the volume of dry particle.
[b] SDS: sodium dodecyl sulphate (0.2 wt % aqueous SDS solution).

porogen. Comparing the properties of beads and bulk samples, it should be brought in mind that there are several important differences between "suspension-like" bead preparation and the quiescent bulk polymerization. The most important differences are lack of interfacial tension in bulk polymerization as the bulk has no aqueous phase, and dynamic forces are also absent in the case of bulk preparation. It is not unlikely that these physical phenomena may have an effect on the phase separation, network formation and final structure characteristics.

It is known that after one vinyl group has reacted, the reactivity of the second double bond decreases.[8] The growing macroradical comes into contact not only with monomer molecules, but also with pendant vinyls. An increased local concentration of pendant vinyls may lead to the formation of intramolecular connections. The inert diluent does not practically affect the local concentration of pendant vinyl groups, but lowers the concentration of monomer so that the participation of pendant vinyl groups in the intramolecular reaction increases comparatively. Thus, a strong cyclization effect is characteristic for the copolymerization of bis-unsaturated monomer especially in the early stages of reaction. Cyclization has been shown to increase upon increasing dilution and by increasing the amount of the crosslinking agent. It is also found to be dependent on the solvating quality of the diluent.[23,24]

It is known from the literature that the second vinyl group of *para*-DVB is less reactive than styrene in the radical copolymerization with styrene.[25] Linear chains of poly(*para*-DVB) have also been prepared by anionic polymerization due to the low reactivity of the second double bond of *para*-DVB compared with *meta*-DVB.[26] The differences in residual vinyl group content also may be a result of steric restrictions during the formation of network structures of poly(*para*-DVB) and poly(*meta*-DVB) not taking part in extensive crosslinking.

Swelling

The swelling/shrinking behavior of the macroporous particles has been determined by measuring the optical diameters of dry particles and particles swollen in SDS solution and toluene. The results given in Table II show that particles prepared with toluene as porogen exhibit shrinking/swelling degree in toluene of 27% (v/v) and 58% (v/v) for poly(*meta*-DVB) and poly(*para*-DVB), respectively. Dry particles when immersed in toluene swell spontaneously until the target diameter is reached. The swelling also leads to an increase in internal pore sizes over that measured on dry

Table III   Porous Properties of Monodisperse Polymer Particles and Bulk Samples

Sample	Total V_g (cm³/g)	S_g (m²/g)	Pore Size Distribution (cm³/g)		
			< 50 Å	50–500 Å	500–5000 Å
A1E	1.62	1043	0.72[a]	0.89	0.01[b]
A2E	1.12	916	0.91[a]	0.20[a]	0.01[b]
A4E	2.25	515	0.27	0.15	1.83
A5E	2.25	546	0.31	0.81	0.89
A14	2.30	457	0.32	0.18	1.80
A15	2.06	598	0.35	0.83	0.89
A16	2.05	1067	0.60[a]	1.45[a]	0.00[b]
A17	1.44	1025	0.72[a]	0.72[a]	0.00[b]

[a] Differential pore volume determined by nitrogen desorption.
[b] Differential pore volume determined by nitrogen desorption and mercury porosimetry.

beads. This is confirmed by the inverse size exclusion chromatography experiments shown in the present paper. The particles prepared with 2-EHA as porogen show no shrinking or swelling behavior.

Looking at the values in Table I for residual vinyl groups in monodisperse particles, one would assume a similar degree of crosslinking in matrices prepared from the same isomeric monomer regardless of diluent type. This does not necessarily mean similar structures as it is impossible to distinguish between intermolecular and intramolecular crosslinking by any of the characterization methods applied. The large differences in the swelling behavior between beads prepared with toluene (good solvent) and 2-EHA (poor solvent) have to be ascribed to a different progress of the crosslinking reaction and the building of the porous structure. It is found that the incipience of phase separation occurs at quite different degrees of conversion dependent upon the porogen type.[15]

According to Huxham et al.,[27] samples prepared with pure *para*-DVB in the presence of toluene give rise to a rapid generation of a highly rigid, strained, and dense matrix of crosslinked polymer chains at low conversion. At high proportions of toluene the whole process of pore formation is probably increasingly delayed by the more extensive solvation of the macromolecular matrix, resulting in the formation of smaller pores. The formed nuclei will be well individualized and linked only by flexible quasilinear molecules. Upon drying, these molecules undergo high stress and then shrink so that the interstitial pores between the nuclei become very small. Upon swelling, the connecting molecules can expand creating rather large pores between the swollen nuclei.[12]

Pore Size Distribution

Table III shows the pore size distribution, total pore volume (V_g) and specific surface area (S_g) of the porous samples based on nitrogen desorption isotherm and mercury porosimetry. The cumulative pore size distribution determined by both nitrogen desorption isotherm and mercury porosimetry of A1E, A2E, A4E, and A5E is given in Figure 1(a–d). Large deviations between these two methods appear for the pore size range 50–1000 Å for both A1E and A2E, resulting in a higher cumulative pore volume from nitrogen desorption within this pore size range.

Mercury penetration is a well-established method for the determination of pore size distribution for pore sizes 200–10,000 Å, while nitrogen adsorption is suitable for the measurement of micropores (<20 Å) and mesopores (20–500 Å) with a practical upper limit of 250 Å radius based upon the classification adopted by IUPAC.[28] According to Cheng et al.,[28] these two methods are best regarded as complementary, for each becomes uncertain as the pore size range approaches a limit, nitrogen adsorption at the upper end of the mesopore range and mercury at the lower end. The very high pressure involved in the detection of small pores with mercury porosimetry may raise the potential problem of collapse of the polymer matrices. Therefore, when samples are exposed to increasing pressure of mercury during the pore size measurements, the polymer matrices are likely to be compressed.[28] Due to this uncertainty, the pore size distribution (10–2000 Å) of A1E and A2E is based on the nitrogen desorption isotherm (Table III). In the case of the macroporous particles prepared with 2-EHA, there is a good agreement between the mercury porosimetry and nitrogen desorption isotherm in the pore size range 50–200 Å [Fig.1(c,d)]. The theoretical total pore volume for the four different particle types is 2.10 mL/g, calculated as the porosity of dry particles where the porogen only is responsible for the pore formation. The total pore volume of A1E and A2E determined by nitrogen desorption isotherm is 77 and 54%, respectively, of the theoretical value, while corresponding values of A4E and A5E are in good agreement with the theoretical values. The observed deviation between the theoretical and measured value of the total pore volume of particles prepared with toluene as pore-forming agent, may be explained by the shrinking behavior upon drying, as shown in Table II.

Large differences in the pore size distribution are obtained for the four types of particles by varying the type of DVB isomer (*meta* vs *para*) and porogen type (toluene vs 2-EHA). The macroporous particles with toluene as porogen contain mainly small- (<50 Å) and medium-sized pores (50–500 Å), but particles composed of poly(*meta*-DVB) have a higher fraction of medium-sized pores and a smaller fraction of small pores than particles of poly(*para*-DVB). Both of these particle types have a high surface area mainly due to the large fraction of small pores. In contrast to the particles prepared with toluene as porogen, the macroporous particles made in the presence of 2-EHA have a substantial fraction of large pores (500–5000 Å). Monosized beads of poly(*meta*-
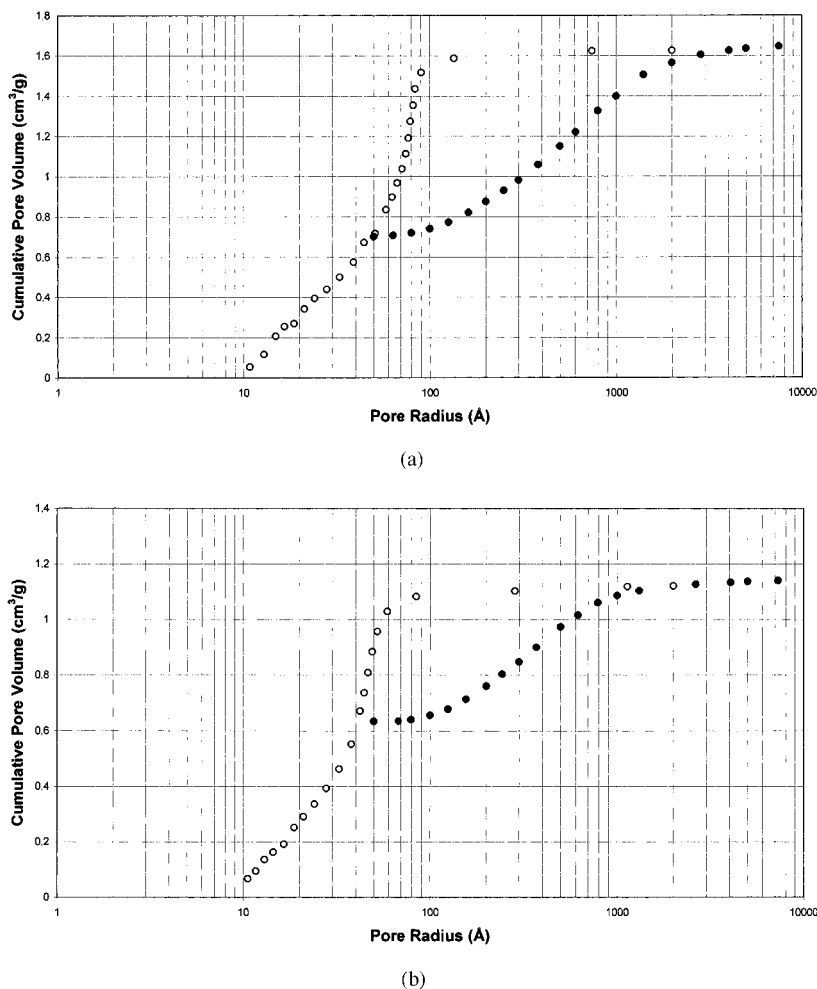
(a)

(b)

Figure 1 Cumulative pore size distribution of monosized particles. Nitrogen desorption isotherm (open circles) and mercury porosimetry (filled circles). (a) A1E [poly(*meta*-DVB)/toluene], (b) A2E [poly(*para*-DVB)/toluene], (c) A4E [poly(*meta*-DVB)/2-EHA], and (d) A5E [poly(*para*-DVB)/2-EHA].

DVB) formed in 2-EHA have a bimodal pore size distribution with a considerable fraction of small pores (<50 Å) and a large fraction of pores between 500 and 5000 Å. A similar pore size distribution has been obtained for styrene–DVB copolymers with 60% DVB (commercial DVB mixture) prepared with 2-EHA.[29] In the present study, the pore size distribution is changed from a bimodal to a polymodal distribution when the monomer is changed from *meta*-DVB to *para*-DVB in the presence of 2-EHA. Particles of poly(*meta*-DVB) and poly(*para*-DVB) prepared with 2-EHA have quite large surface areas, but the values are much lower than for the corresponding matrices with toluene as porogen.

The cumulative pore size distribution as determined by nitrogen desorption isotherm and mercury porosimetry of the bulk samples A16 and A17 prepared with toluene is shown in Figure 2(a,b). There is a deviation between these two methods similar to the one observed for A1E and A2E, which indicates that the bulk samples prepared with toluene as porogen also are built up of a nonrigid porous structure that may be compressed by the high pressure of mercury applied in the determination of smaller pore sizes. Bulk samples prepared with toluene as porogen (A16 and A17) consist mainly of small pores (<50 Å) and medium-sized pores (50–500 Å) as shown in Table III. The pore volume in the pore size range 50–500 Å and the total pore volume are both higher for the bulk samples (A16 and A17) compared with the monosized particles with the same composition (A1E and A2E). The small differ-
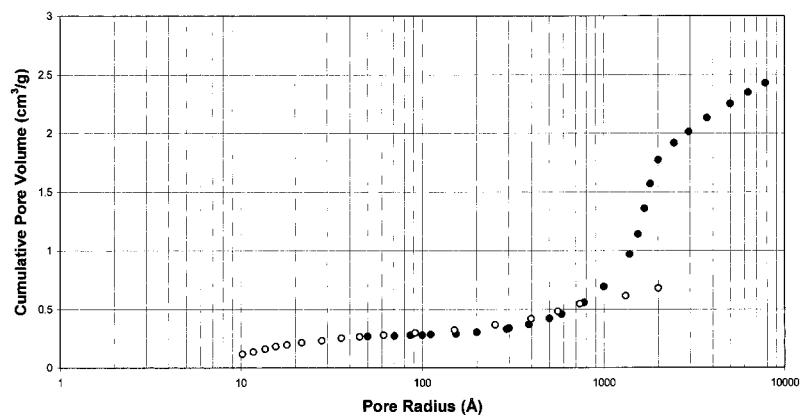
(c)
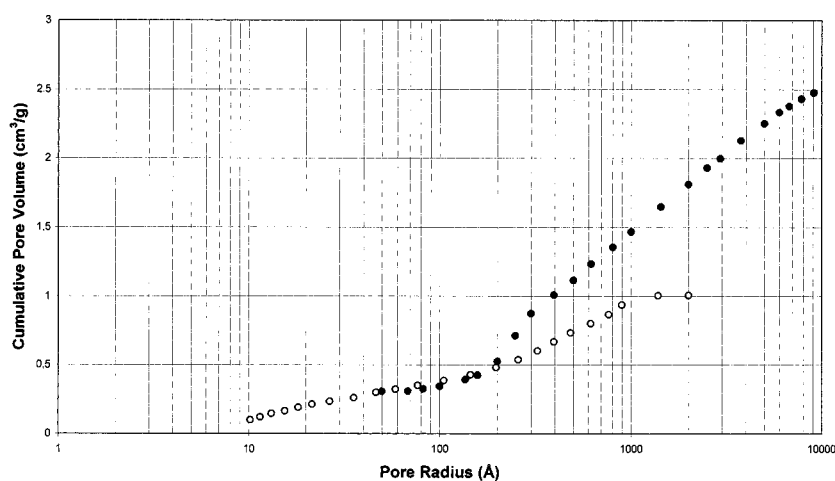
(d)

**Figure 1**   (*Continued from the previous page*)

ences in the pore size distribution of these crosslinked polymers in the dry state may be attributed to the higher total pore volume, which again may be due to the swelling/shrinking behavior that may differ from bulk samples to monosized particles. The cumulative pore size distribution of A14 and A15 prepared with 2-EHA (table 3) determined by mercury porosimetry shows very good agreement with the pore size distribution of the corresponding monosized polymer particles.

There are some important differences in the preparation method of bead and bulk samples as discussed above. Svec and Frechet[30,31] have found a median pore diameter of 85 nm for beads while it is 315 nm for the rod. The dynamics of the system resulting from stirring seem to be the main cause for the difference in pore size distri-

bution between the molded rods and classical beads. In the present study, bulk samples and monosized particles show the same characteristics with regard to the pore size distribution, specific surface area, and amount of residual vinyl groups, and no large differences between monosized beads and bulk samples have been observed.[30,31]

Bromination

The surface area S_g of the different particles of various degrees of bromination was determined by the BET isotherm. The results are given in Table IV together with a calculated surface area S_{gw} based on the surface area of unbrominated particles corrected for the weight gain due to bromine addition.
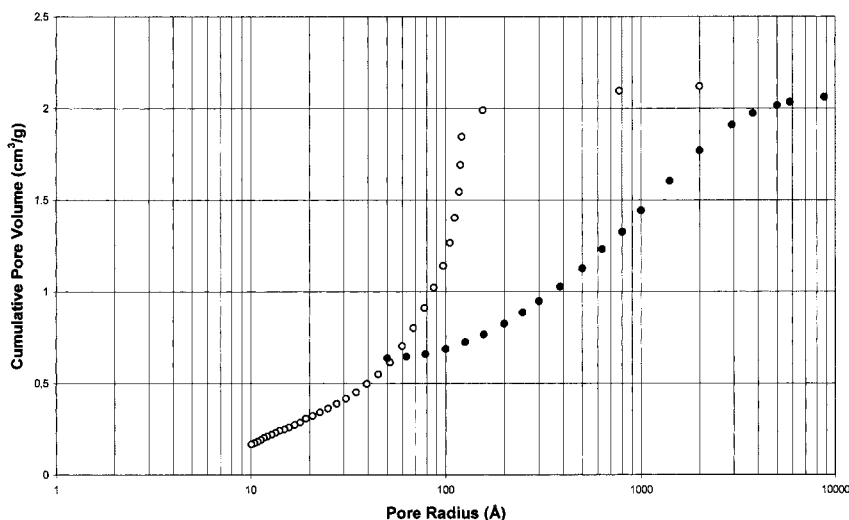
(a)
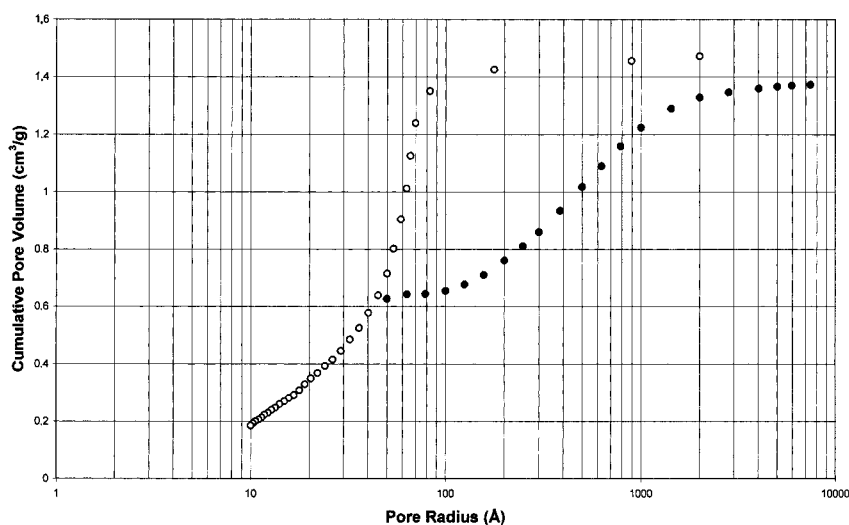
(b)

Figure 2 Cumulative pore size distribution of bulk samples. Nitrogen desorption isotherm (open circles) and mercury porosimetry (filled circles). (a) A16 [poly(*meta*-DVB)/toluene] and (b) A17 [poly(*para*-DVB)/toluene].

It is seen that particles prepared from *meta*- and *para*-DVB with toluene as porogen show a quite good agreement between the measured (S_g) and the calculated (S_{gw}) surface areas. The calculated values S_{gw} are always higher than the measured ones except for A2E2B and A2E3B, which show a rather small difference in the opposite direction. The difference between S_g and S_{gw} increases with increasing bromine content of the particles. At the lowest degrees of bromination, the difference is about 2–3% and increases to 13 at 36% bromine content (A2E1B).

In addition to the effect of weight increase on the surface area per weight unit due to bromine addition, it is not unlikely that bromine will reduce the total surface by occupying space while entering or even closing the smallest pores. This may contribute to the difference between S_g and S_{gw}.

A counteracting effect may be that the bromination leads to a higher degree of permanent porosity in the dry state and thereby contribute to a higher surface area. Possibly a reaction between bromine and pendant vinyl groups belonging to

Table IV   Bromine Content and Specific Surface Area of Monosized Polymer Particles

Sample	% Bromine (wt %)	S_g [a] (m²/g)	S_{gw} [b] (m²/g)
A1E	0	1043	
A1E2B	6.9 ± 0.35	947	971
A1E3B	13.7 ± 0.69	883	900
A1E4B	18.6 ± 0.93	798	849
A1E5B	24.5 ± 1.23	717	787
A1E1B	30.5 ± 1.53	660	724
A2E	0	916	
A2E2B	8.0 ± 0.40	859	843
A2E3B	15.5 ± 0.78	791	774
A2E4B	21.9 ± 1.10	681	715
A2E5B	26.6 ± 1.33	619	672
A2E1B	35.8 ± 1.79	521	588
A4E	0	515	
A4E2B	7.6 ± 0.38	431	475
A4E3B	13.6 ± 0.68	353	445
A4E4B	18.4 ± 0.92	284	420
A4E5B	24.7 ± 1.24	188	388
A4E1B	30.6 ± 1.53	122	356
A5E	0	546	
A5E2B	7.7 ± 0.39	460	504
A5E3B	15.5 ± 0.78	345	461
A5E4B	23.0 ± 1.15	274	420
A5E5B	30.5 ± 1.53	221	379
A5E1B	36.0 ± 1.80	177	349

[a] S_g: specific surface area (m²/g) determined by BET isotherm.
[b] S_{gw}: calculated specific surface area (m²/g) corrected for weight increase due to bromination.

quasilinear chains connecting the nuclei may impose an increased strain or rigidity to these chains leading to a decreased shrinkage upon drying.

For particles prepared with 2-EHA as porogen there are large differences between the values of S_g and S_{gw}. At a bromine content of 30 wt % introduced into particles of poly(*meta*-DVB), the calculated surface area S_{gw} is about 3 times higher than the measured BET value S_g, while particles from *para*-DVB with a bromine content of 36 w t% have S_{gw} values about 2 times higher than S_g. Most probably some of the smallest pores are filled up or blocked as a result of bromine addition.

The results of bromination of the bulk samples are given in Table V. It will be seen that corresponding particles and bulk samples give quite similar results, and there are only some minor differences. As said earlier, deviations may occur due to differences in the preparation method between bead and bulk samples.

As particles prepared with 2-EHA as porogen show neither shrinking nor swelling in organic solvents, it is not unlikely that the reaction with bromine in this case takes place primarily at the pore surfaces. This again indicates that the pendant vinyls are not buried within compact domains of the matrices. The situation may not be the same when the particles are prepared in the presence of a good solvent like toluene, as such particles may be swollen in organic solvents and by the bromination liquid. In the latter case it may be expected that also vinyl groups buried in the solid material of the matrices could be brominated.

In case the remaining vinyl groups are supposed to be located on the pore surfaces, one may calculate the average available area per pendant vinyl group applying measured values given in Tables I and III. The calculated results for both beads and bulk samples given in Table VI show an available surface area for all samples in the range 26–65 Å² per vinyl group. The bromine reaction involves the formation of a bromonium ion and theoretically the calculated average spacing between the vinyl groups should be sufficiently high to allow the bromine addition to take place.[17,18] It is stressed that the the total amount of vinyl groups determined by infrared spectroscopy, FTIR, also given in the present paper, is in good accordance with the values obtained by bromination confirming the feasibility of the bromine method.

Table V   Bromine Content and Specific Surface Area of Bulk Samples

Sample	% Bromine (wt %)	S_g [a] (m²/g)	S_{gw} [b] (m²/g)
A16	0	1067	
A161B	30.2 ± 1.51	626	745
A17	0	1025	
A171B	37.2 ± 1.86	575	644
A14	0	457	
A141B	24.6 ± 1.23	133	345
A15	0	598	
A151B	33.6 ± 1.68	274	397

[a] S_g: specific surface area (m²/g) determined by BET isotherm.
[b] S_{gw}: calculated specific surface area (m²/g) corrected for weight increase due to bromination.

Table VI Average Area per Pendant Vinyl Group

Sample	Area per Pendant Vinyl Group ($Å^2$/vinyl group)
A1E	63.0
A2E	43.6
A4E	31.0
A5E	25.8
A14	37.2
A15	31.3
A16	65.4
A17	45.9

Inverse Size Exclusion Chromatography

ISEC calibration curves obtained for the four different particle types are given in Figure 3. Values of the pore diameter (D) are calculated from the molecular weight (M_w) of polystyrene standards according to the empirically derived eq. (3)[32] :

$$D = 0.62 \cdot M_w^{0.59} \tag{3}$$

Particles of poly(*meta*-DVB) and poly(*para*-DVB) prepared in the presence of toluene show linear calibration curves with separation of molecules with molecular weight up to 96,000 g/mole. There is no separation of polystyrene standards above 96,000 molecular weight. This indicates a lack of pores with diameters larger than 600 Å. The larg-

est pore radius measured by nitrogen desorption in the dry state was respectively 150 and 100 Å for A1E and A2E. In the presence of a solvent (tetrahydrofuran) the largest pore radius is shifted to 300 Å. These results confirm the swelling/shrinking behavior of these samples. The calibration curves show that 30% of the porosity of A1E and A2E is available to molecules with a molecular weight larger than 10,000. The macroporous particles made with 2-EHA as pore-forming agent show an increased selectivity for the higher molecular weight solutes that can be attributed to the presence of larger pores. The presence of large pores in A4E and A5E is also confirmed by SEM, AFM, and pore size distribution measurements. An upper exclusion limit above 10^7 is obtained for A4E. These samples show a poor separation of molecules of molecular weights below 5000 g/mole compared to particles prepared in toluene. In comparison, 80% of the porosity of A4E and A5E is available to molecules larger than 10,000 in molecular weight.

The calibration curves obtained for the beads prepared with toluene as porogenic agent are almost straight lines, indicating the presence of one type of pores in these materials. The calibration curves of the macroporous particles prepared in the presence of 2-EHA as porogen are not straight lines in the whole molecular weight range. A4E particles are able to separate polystyrenes of molecular weights in the whole range despite the fact that the pore size distribution from nitrogen
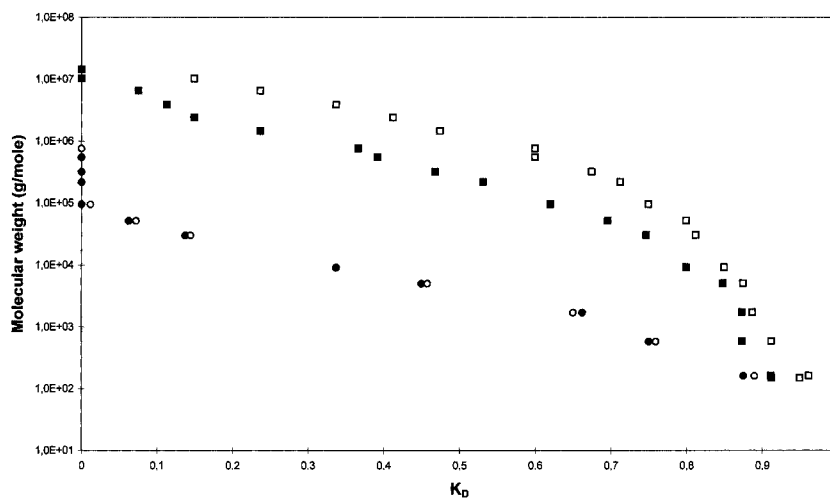

Figure 3 Inverse size exclusion calibration curves of macroporous, monosized particles. A1E [poly(*meta*-DVB)/toluene] (open circles), A2E [poly(*para*-DVB)/toluene] (filled circles), A4E [poly(*meta*-DVB)/2-EHA] (open quadrangles), and A5E [poly(*para*-DVB)/2-EHA] (filled quadrangles).
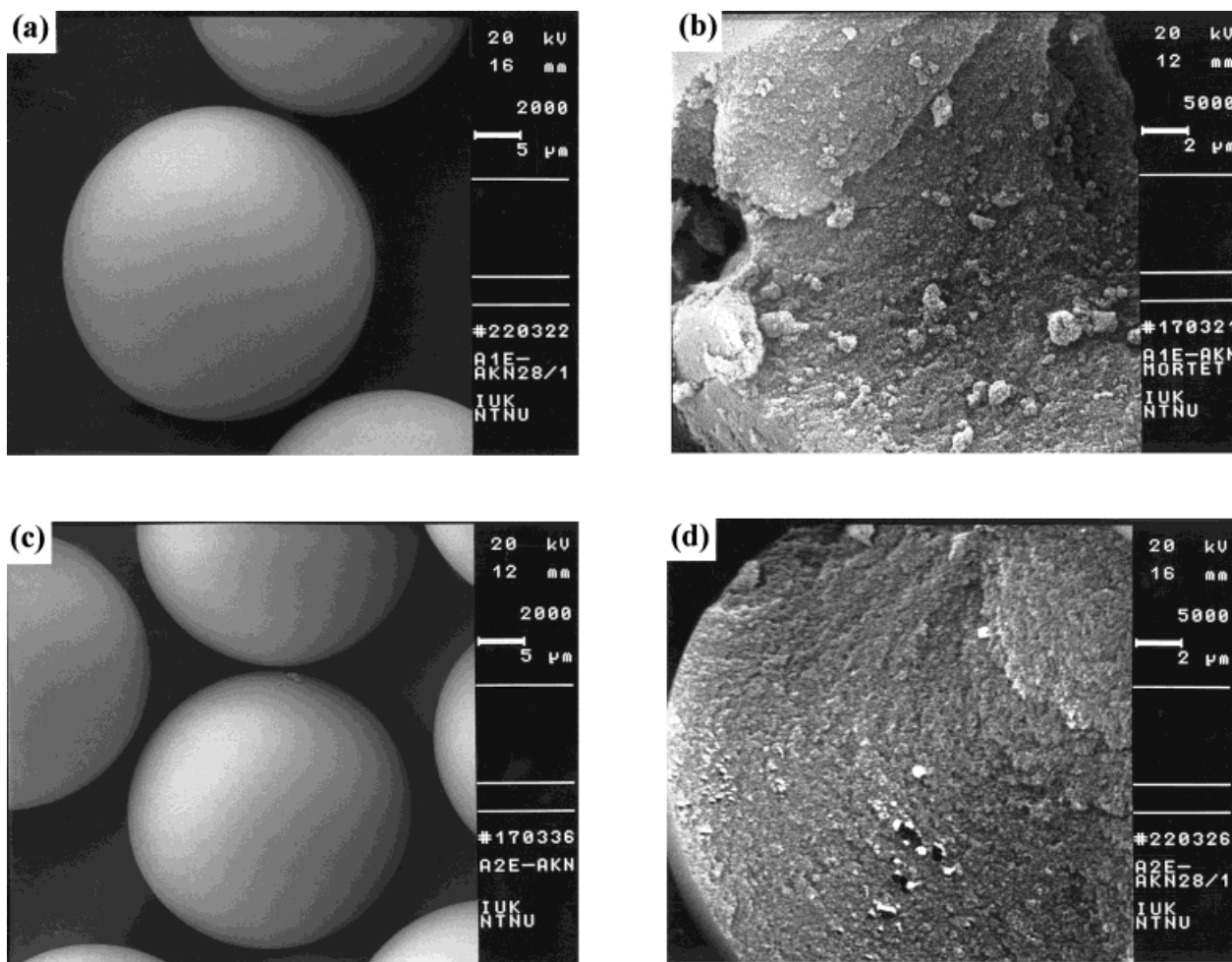
Figure 4 Scanning electron micrographs of 33 μm monosized polymer particles. (a) A1E [poly(*meta*-DVB)/toluene] (2000×), (b) A1E [poly(*meta*-DVB)/toluene] fractured bead (5000×), (c) A2E [poly(*para*-DVB)/toluene] (2000×), (d) A2E [poly(*para*-DVB)/ toluene] fractured bead (5000x), (e) A4E [poly(*meta*-DVB)/2-EHA] (2000×), (f) A4E [poly(*meta*-DVB)/2-EHA] (10,000×), (g) A5E [poly(*para*-DVB)/2-EHA] (2000×), and (h) A5E [poly(*para*-DVB)/2-EHA] (10,000×).

desorption and mercury porosimetry on dry samples show an almost complete lack of pores in the region 50–300 Å. Poly(*meta*-DVB) and poly(*para*-DVB) particles of 18 μm prepared with toluene as porogen, which were packed in stainless steel columns of dimension 150 × 4.6 mm i.d. at 1.0 mL/ min flow, gave identical calibration curves (not shown) to A1E and A2E packed in glass columns of dimension 34 × 10 mm i.d.

Scanning Electron Microscopy

The texture of the four particle types investigated by SEM is given in Figure 4. SEM micrographs of monosized particles of poly(*meta*-DVB) and poly(*para*-DVB) prepared in toluene [Fig. 4(a,c)] reveal a very smooth surface. SEM micrographs [Fig. 4(b,d)] of the interior of the particles (fractured beads)] show a very homogeneous fine-porous structure throughout the beads. There are large differences in the morphology between A4E and A5E as shown in Figures 4(e) and 4(g). The samples of A4E show a very rough heterogeneous surface with the presence of large pores penetrating the particles. When the monomer is changed from *meta*-DVB to *para*-DVB, resulting in A5E, the surface becomes less rough (than A4E) with a more uniform distribution of smaller pores compared to A4E. The differences in apparent pore size distribution and morphology between A4E
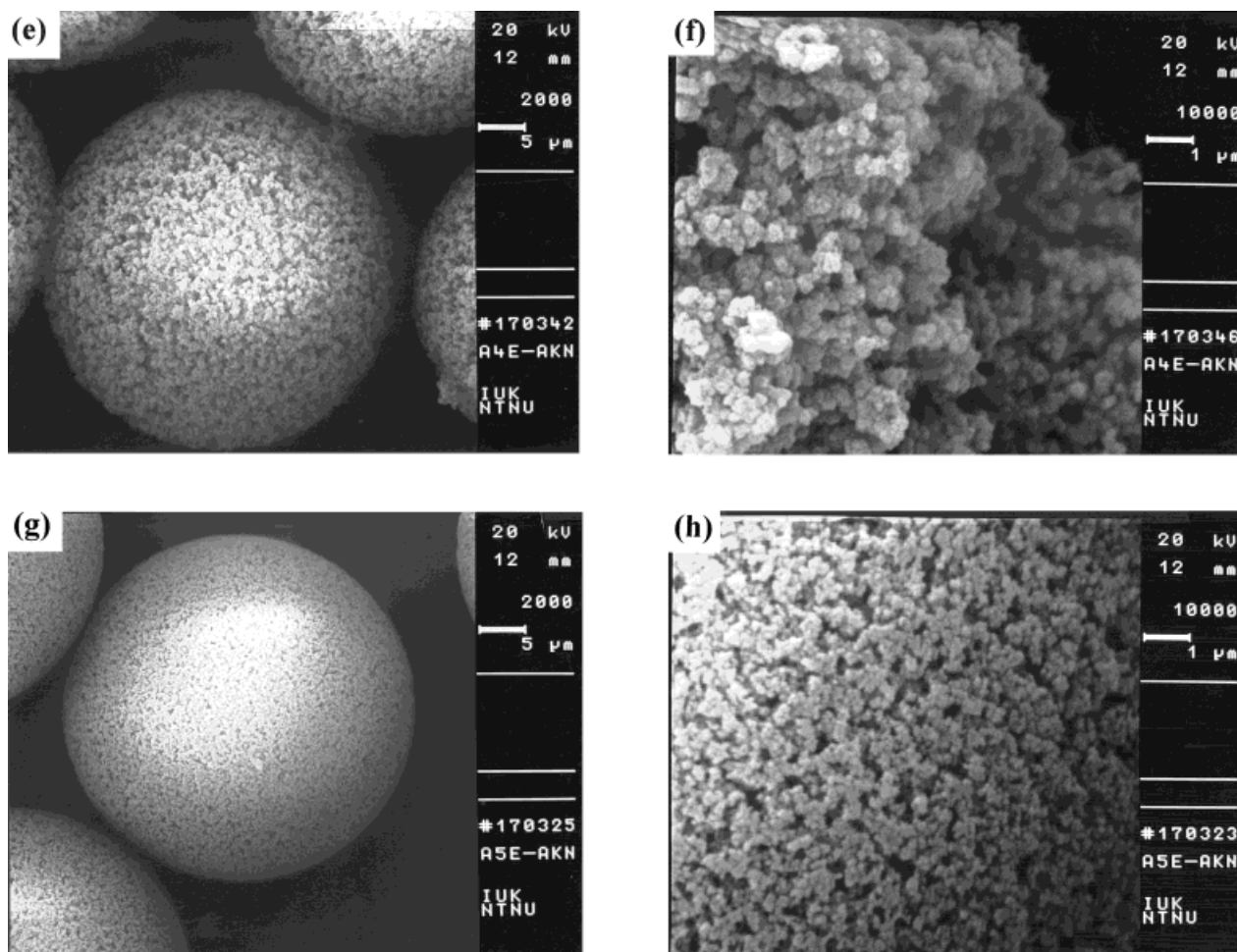
Figure 4   (*Continued from the previous page*)

and A5E observed from SEM are also confirmed by the mercury porosimetry measurements.

A previous study of styrene–DVB copolymers with 2-EHA as porogenic agent has shown that the texture consists of nuclei, microspheres, and large aggregates of microspheres.[29] It was concluded that the size of the microspheres decreased and that they tended to be slightly fused with decreasing DVB content. When the microspheres were becoming more fused, the intermediate pores tended to disappear. The change in surface morphology from A4E to A5E indicates that phase separation has occured at a later stage of the polymerization of *para*-DVB than *meta*-DVB in 2-EHA. Images of A2E and A5E with a larger magnification (×75,000) are given in Figure 5. From an examination of the micrograph of a fractured A2E particle, a uniform distribution of agglomerates of medium-sized nodules (200–800 Å) and a dense structure can be observed. A5E con-sists of agglomerates of microspheres (1000 Å) that look like cauliflowers with large pores between the agglomerates. The distribution of the agglomerates is more nonuniform than of A2E and has a less dense structure. These observations are in accordance with the mechanism for the pore formation proposed by Guyot[12] and Kun and Kunin[2] in the presence of a good solvent and a poor solvent. The calculated size of the nuclei/microspheres according to eq. (1) based on the skeletal density given in Table VII is 52Å (A1E), 59Å (A2E), 104Å (A4E), and 97Å (A5E).

Atomic Force Microscopy

Atomic force microscopy analysis have been performed on the four types of monosized particles. The three-dimensional images of the A1E, A2E, A4E, and A5E samples are shown in Figure 6(a–d). The scan sizes are: $1 \times 1 \ \mu m \times 100$ nm for A1E
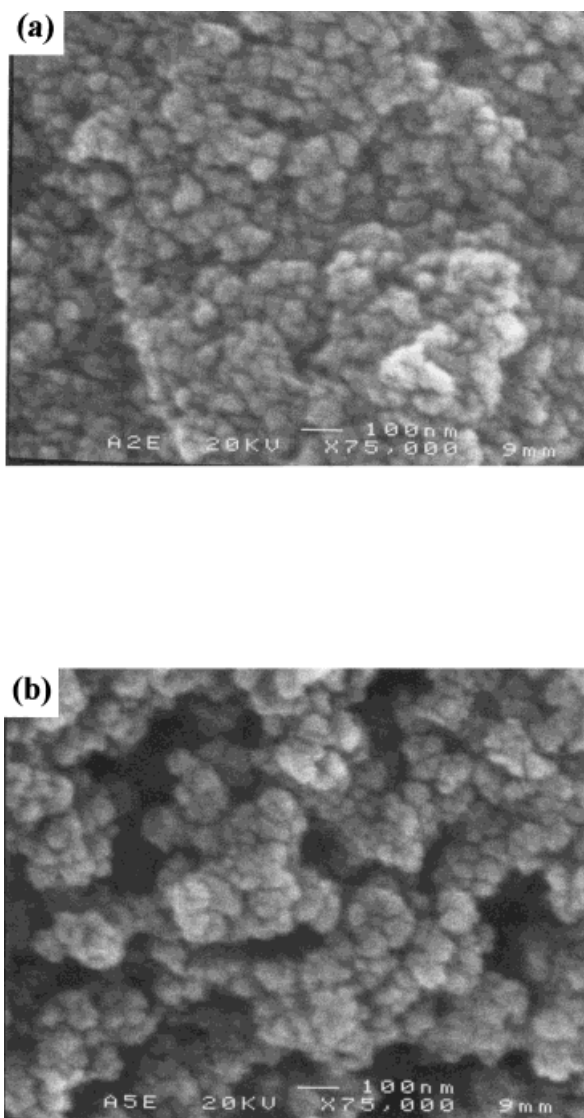
Figure 5 Scanning electron micrographs of 33 μm monosized polymer particles (a) A2E [poly(*para*-DVB)/toluene] (75,000×) and (b) A5E [poly(*para*-DVB)/2-EHA] (75,000×).

and A2E and 1×1 μm $\times$ 750 nm for A4E and A5E. The light areas correspond to the maximal heights in the Z direction, and the dark areas are related to the minimal heights. From the images it seems that the macroporous particles formed in the presence of toluene exhibit very smooth surfaces, where A2E seems to have a more dense structure than A1E. Pore size distribution measurements have also indicated that A1E has a higher content of pores between 50 and 500 Å than A2E. The topography appears to be different for these samples, in which A2E seems to have a more uniform and less rough surface. The macro-

porous particles made with 2-EHA have rough surfaces with large pores penetrating the particles. This gives rise to a topography different from A1E and A2E. A4E seems to have the most macroporous morphology with a nonuniform distribution of large agglomerates of microspheres that appear to have been coalesced and fused together during the polymerization, and wide and deep rifts are observed. The samples made of poly(*para*-DVB) in 2-EHA also consist of large agglomerates of microspheres, but in contrast to A4E the spherical shape of the individual microspheres is retained during the polymerization. A5E samples also have a more uniform distribution of large agglomerates. From these observations one can assume that the phase separation in 2-EHA occurs at an earlier stage for *meta*-DVB than for *para*-DVB.[15]

The roughness parameters for the different particle types are given in Table VIII and show large differences between the samples. The data show an increasing roughness of the particles in the order A2E < A1E < A5E < A4E. The roughness parameters depend on the curvature and the size of the TM AFM tip as well as the treatment of the captured surface data (plane fitting, flattening and filtering), and they should not be considered as absolute roughness values.

FTIR

DRIFT spectroscopy is used to quantify the relative amount of residual vinyl groups in poly(*meta*-DVB) and poly(*para*-DVB) particles. The FTIR spectra (in KM units) of poly(*meta*-DVB) and poly(*para*-DVB) particles prepared with toluene or 2-EHA before and after bromination (in excess) are shown in Figure 7(a–d). The peak assignments are given in Table IX. Bartholin et al.[33] have developed a method for a quantitative determination of vinyl group content in co-(polystyrene–DVB) beads by infrared analysis. Since the

Table VII   Skeletal Density of Monosized Polymer Particles

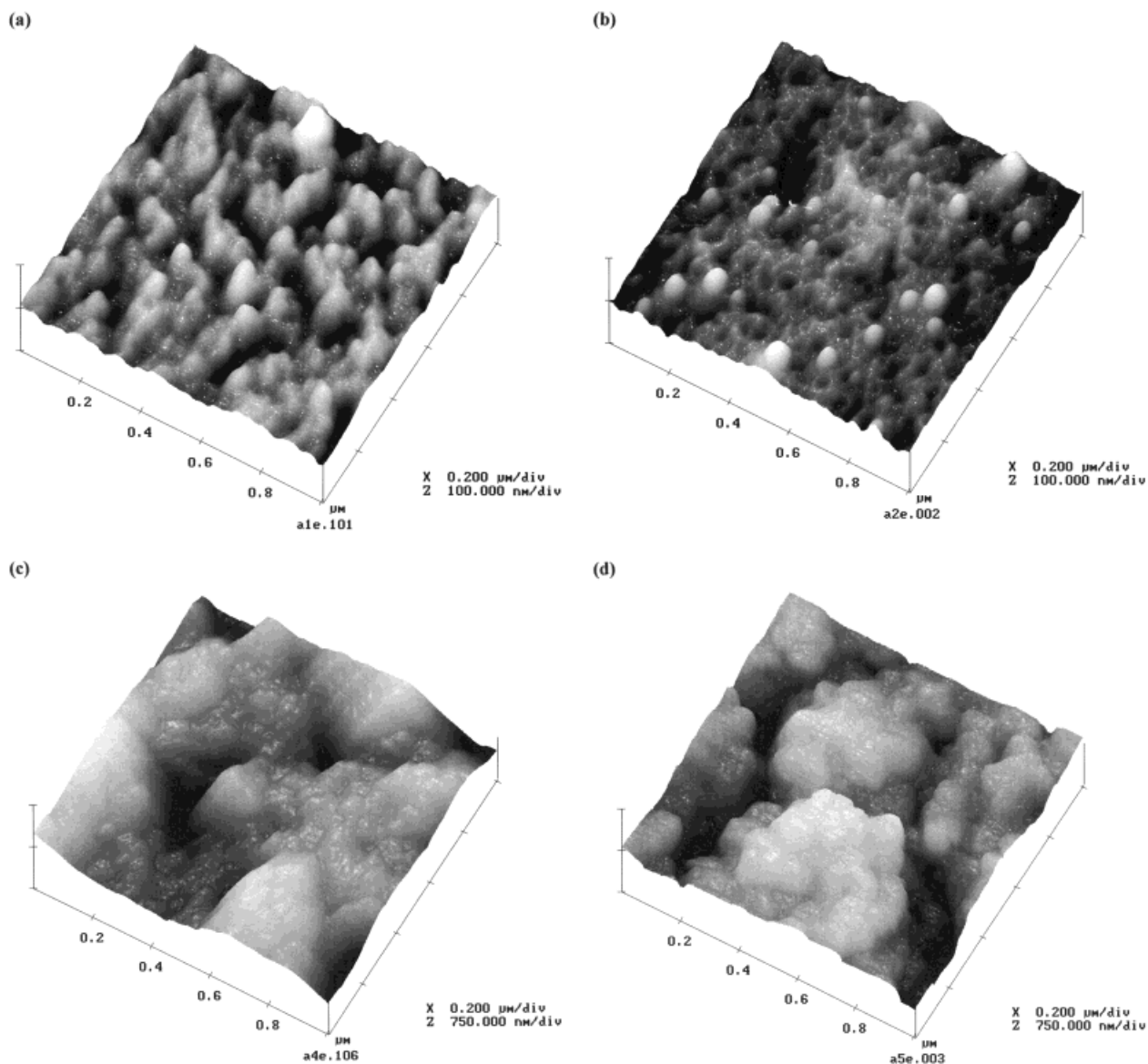| Sample	Skeletal Density, ρ_s (g/cm^3)
A1E	1.11
A2E	1.10
A4E	1.12
A5E	1.13

Figure 6 Atomic force images of 33 μm monosized polymer particles (a) A1E [poly-(*meta*-DVB)/toluene], (b) A2E [poly(*para*-DVB)/toluene], (c) A4E [poly(*meta*-DVB)/2-EHA], and (d) A5E [poly(*para*-DVB)/2-EHA].

particles in this study are homopolymers of either *meta*-DVB or *para*-DVB, a modified method reported by Hubbard et al.[34] has been applied. The content of vinyl groups (X_{vb}: % double bonds) is calculated according to

$$X_{vb} = \frac{(A + B)}{2(C + D)} \times 100\% \qquad (4)$$

The peak heights multiplied by their various extinction coefficients give A, B, C, and D.[33] The vinyl peaks are at 1630 cm^{-1} (A) and 990 cm^{-1}

(B), and the *para*-disubstitued phenyl ring is at 1510 cm^{-1} (C) and *meta*-disubstituted phenyl ring is at 795 cm^{-1} (D). C and D account for all of the repeat units in the polymer. For the polymer matrices investigated in this study either C or D is used. In the present study A, B, C, and D represent the peak heights in Kubelka Munk units multiplied by the various extinction coefficients given by Bartholin et al.[33] It is assumed that the relative ratio between the extinction coefficients in transmission spectroscopy and DRIFT spectroscopy remains constant. According

Table VIII   Roughness Parameters of Monosized Polymer Particles from AFM Analysis

Sample	$R_a{}^a$ (nm)	$R_{max}{}^b$ (nm)	$R_q{}^c$ (nm)
A1E	7.7	142.8	10.3
A2E	6.4	95.4	8.9
A4E	198.8	1383.0	248
A5E	101.6	912.5	127.5

[a] R_a: mean roughness relative to the centerplane.
[b] R_{max}: Difference in height between the highest and lowest plane points relative to the mean plane.
[c] R_q: root mean square of the Z data.

to Hubbard et al.,[34] the degree of crosslinking is calculated by

$$X_{cl} = \% \text{ DVB} - X_{vb} \qquad (5)$$

where X_{cl} is degree of crosslinking and %DVB is the divinylbenzene content (100% in this study). The vinylbenzene content in mmole/g is calculated by multiplying X_{vb} with the vinyl group content of a linear poly(DVB) chain, which is 7.7 mmole/g. The calculated values for the four different particle types before and after the bromination are shown in Table X. The conversion of the second double bond from IR that corresponds to the degree of crosslinking is calculated to be 63.8% (A1E), 48% (A2E), 61.1% (A4E), and 52% (A5E), and the values of the vinyl group content obtained in this study are in the same range as those found by Hubbard et al.[34] The residual vinyl group content determined by FTIR is in good agreement with the values determined from bromination (Tables I and X) and the vinyl group content in poly(*para*-DVB) matrices is slightly higher than calculated from the bromination reaction. The content of residual vinyl groups as
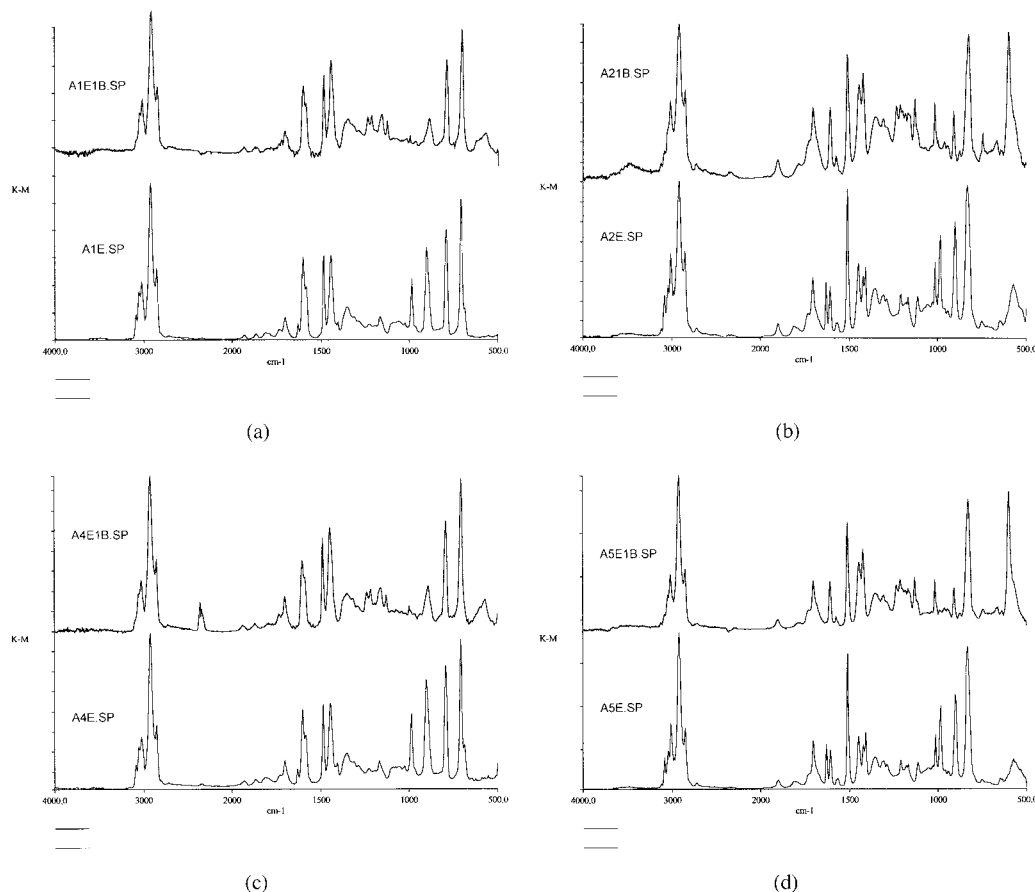

Figure 7   Diffuse reflectance FTIR spectra of monosized polymer particles prior and after bromination (a) A1E [poly(*meta*-DVB)/toluene], (b) A2E [poly(*para*-DVB)/toluene], (c) A4E [poly(*meta*-DVB)/2-EHA], and (d) A5E [poly(*para*-DVB)/2-EHA].

Table IX   Peak Assignments of FTIR Spectra of Unbrominated and Brominated Poly(*meta*-DVB) and Poly(*para*-DVB) Particles

Weavenumber (cm^{-1})	Peak Assignment
3010–3110	Aromatic CH
2925	Aliphatic CH$_2$
2855	Aliphatic CH$_2$
1705	Carbonyl
1660–2000	Characteristic overtone patterns
1630	RCH=CH$_2$
1600	Aromatic C—C
1486	Aromatic C—C (*meta*)
1510	Aromatic C—C (*para*)
1450–1475	RCH$_3$, RCH$_2$R'
990	RCH=CH$_2$
905	RCH=CH$_2$
795	1,3-Disubstituted aromatic
709	1,3-Disubstituted aromatic
836	1,4-Disubstituted aromatic
1236, 1216, 1130, 1183	(1,2-Dibromoethyl)benzene
602	(1,2-Dibromoethyl)(*para*-DVB)
571	(1,2-Dibromoethyl)(*meta*-DVB)

determined by bromination may be too low if some of these groups are buried and not available for the bromination reaction. The fraction of deeply hidden double bonds not available for reactions is expected to increase with increasing degree of crosslinking.[3] From IR spectra, however, only negligible amounts of residual vinyl groups are left after the bromination reaction of A1E and A4E. This indicates that almost all of the

pendant vinyl groups have been accessible for bromination. A higher reactivity of the second double bond of *meta*-DVB than of *para*-DVB may lead to a higher fraction of unreacted groups buried inside the nuclei due to an earlier precipitation of the crosslinked polymer.[15] However, the observed deviations between IR and bromination are very small.

CONCLUSIONS

Monodisperse poly(*meta*-divinylbenzene) and poly(*para*-divinylbenzene) beads prepared by the two-step activated swelling method with large differences in the porous properties have been prepared. A change in porogen from toluene to 2-ethylhexanoic acid leads to an increase in both pore size and pore volume in the dry state. Different pore size distribution is also obtained with the change from *meta*-DVB to *para*-DVB with 2-ethylhexanoic acid as porogen. The change of DVB isomer has only a slight influence on the pore size distribution when toluene is used as porogen. The beads prepared with toluene as porogen exhibit a shrinking/swelling behavior in the dry and wet state. When these beads are applied as separation medium in inverse size exclusion chromatography, they show an upper exclusion limit of 96,000 g/mole, which is higher than expected from the pore size distribution in the dry state. Swelling of the beads leading to an increase in the maximum pore size is also observed from ISEC analysis. Beads prepared from *meta*-DVB in the presence of 2-EHA exhibit good separation of narrow polystyrene standards of molecular weights in the range

Table X   Vinyl Group Content of Poly(*meta*-DVB) and Poly(*para*-DVB) Particles Prior and After Bromination by Diffuse Reflectance FTIR

Sample	Vinylbenzene Content[a] X_{vb} (%)	Degree of Crosslinking[b] X_{cl} (%)	Residual Vinyl Groups (mmole C=C/g)
A1E	36.2	63.8	2.78
A1E1B	2.3		0.18
A2E	51.8	48.2	3.98
A2E1B	0		0
A4E	38.9	61.1	2.99
A4E1B	4.2		0.33
A5E	48.0	52.0	3.69
A5E1B	0.4		0.03

[a] Calculated according to eq. (4).
[b] Calculated according to eq. (5).

$5 \cdot 10^3$–10^7 g/mole. The different particle types have a considerable amount of residual double bonds at the end of polymerization as determined by FTIR and bromination. The reductions in the surface area after bromination are higher for poly(*meta*-DVB) than for poly(*para*-DVB) matrices made with 2-EHA as porogen, indicating a different distribution of residual vinyl groups among the various pore sizes. The content of pendant double bonds determined by bromination is consistent with the values found from FTIR for the four particle types studied. SEM and AFM have been valuable tools for investigating the morphology of the samples in this study.

REFERENCES

1. Seidl, J.; Malinsky, J.; Dusek, K.; Heitz, W. Adv Polym Sci 1967, 5, 113.
2. Kun, K. A.; Kunin, R. J Polym Sci Part A-1 1968, 6, 2689.
3. Guyot, A.; Bartholin, M. Prog Polym Sci 1982, 8, 277.
4. Sederel, W. L.; DeJong, G. J. J Appl Polym Sci 1973, 17, 2835.
5. Brooks, B. W. Macromol Chem Macromol Symp 1990, 35/36, 121.
6. Ugelstad, J.; Mørk, P. C.; Herder Kaggerud, K.; Ellingsen, T.; Berge, A. Adv Colloid Interface Sci 1980, 13, 101.
7. Ugelstad, J.; Berge, A.; Ellingsen, T.; Schmid, R.; Nilsen, T. N.; Mørk, P. C.; Stenstad, P.; Hornes, E.; Olsvik, Ø. Prog Polym Sci 1992, 17, 87.
8. Malinsky, J.; Klaban, J.; Dusek, K. J Macromol Sci Chem 1971, A5(6), 1071.
9. Schwachula, G. J Polym Sci Symp 1975, 53, 107.
10. Haupke, K.; Pientka, V. J Chromatog 1974, 102, 117.
11. Chung, D.-Y. D.; Bartholin, M.; Guyot, A. Angew Makromol Chem 1982, 103, 109.
12. Guyot, A. in Syntheses and Separations Using Functional Polymers; Sherrington, D. C., Hodge, P., Eds.; John Wiley: London, 1988; chap 1.
13. Albright, R. L. React Pol 986, 4, 155.
14. Okay, O. Angew Makromol Chem 1987, 153, 125.
15. Nyhus, A. K.; Hagen, S.; Berge, A. J Polym Sci Part A Polym Chem1998, submitted.
16. Siggia, S. in Quantitative Organic Analysis via Functional Groups; Siggia, S., Ed.; Wiley: New York, 1963; p 298.
17. Fukuzumi, S.; Kochi, J. K. Int J Chem Kinetics 1983, 15, 249.
18. Yates, K.; McDonald; R. S.; Shapiro, S. A. J Org Chem 1973, 38, 2460.
19. Brunauer, S.; Emmett, P. H.; Teller, E. J Am Chem Soc 1938, 60, 309.
20. Lowell, S.; Shields, J. E. in Powder Surface Area and Porosity, Lowell, S., Shields, J. E., Eds.; Chapman and Hall: London, 1991; chap 11.
21. Lowell, S.; Shields, J. E. in Powder Surface Area and Porosity, 3rd ed.; Lowell, S., Shields, J. E., Eds.; Chapman and Hall: London, 1991; chap 8.
22. Lehmani, A.; Durand-Vidal, S.; Turq, P. J Appl submitted to Sci 1998, 68, 503.
23. Dusek, K. in Developments in Polymerization; Haward, R. N., Ed.; Applied Science Publishers: London, 1982; chap 4.
24. Heitz, W. Adv Polym Sci 1977, 23, 1.
25. Wiley, R. H.; Jin, J.-I. J Macromol Sci Chem 1969, A3, 835.
26. Nitadori, Y.; Tsuruta, T. Macromol Chem 1978, 179, 2069.
27. Huxham, I. M.; Rowatt, B.; Sherrington, D. C.; Tetley, L. Polymer 1992, 33(13), 2768.
28. Cheng, C. E.; Micale, F. J.; Vanderhoff, J. W.; El-Aasser, M. S. J Colloid Interface Sci 1992, 150(2), 549.
29. Jacobelli, H.; Bartholin, M.; Guyot, A. J Appl Polym Sci 1979, 23, 927.
30. Svec, F.; Frechet, J. M. J Macromol Symp 1996, 110, 203.
31. Svec, F.; Frechet, J. M. J Chem Mater 1995, 7, 707.
32. Halasz, I.; Martin, K. Angew Chem Int Ed Engl 1978, 17, 901.
33. Bartholin, M.; Boissier, G.; Dubois, J. Macromol Chem 1981, 182, 2075.
34. Hubbard, K. L.; Finch, J. A; Darling, G. D. React Funct Polym 1998, 36, 17.